



*Citation for published version:*

Walker, J, Bissas, A, Paradisis, GP, Hanley, B, Tucker, CB, Jongerius, N, Thomas, A, von Lieres und Wilkau, HC, Brazil, A, Wood, MA, Merlino, S, Vazel, PJ & Bezodis, IN 2021, 'Kinematic factors associated with start performance in World-class male sprinters', *Journal of Biomechanics*, vol. 124, 110554.  
<https://doi.org/10.1016/j.jbiomech.2021.110554>

*DOI:*

[10.1016/j.jbiomech.2021.110554](https://doi.org/10.1016/j.jbiomech.2021.110554)

*Publication date:*

2021

*Document Version*

Peer reviewed version

[Link to publication](#)

*Publisher Rights*

CC BY-NC-ND

**University of Bath**

**Alternative formats**

If you require this document in an alternative format, please contact:  
[openaccess@bath.ac.uk](mailto:openaccess@bath.ac.uk)

**General rights**

Copyright and moral rights for the publications made accessible in the public portal are retained by the authors and/or other copyright owners and it is a condition of accessing publications that users recognise and abide by the legal requirements associated with these rights.

**Take down policy**

If you believe that this document breaches copyright please contact us providing details, and we will remove access to the work immediately and investigate your claim.

1 **Article title:** Kinematic factors associated with start performance in World-class male  
2 sprinters

3 **Article type:** Original article  
4

5 **Authors:** Josh Walker<sup>1</sup>, Athanassios Bissas<sup>1,2,3</sup>, Giorgos P. Paradisis<sup>4</sup>, Brian  
6 Hanley<sup>1</sup>, Catherine B. Tucker<sup>1</sup>, Nils Jongerius<sup>1,5</sup>, Aaron Thomas<sup>1</sup>, Hans C. von Lieres und  
7 Wilkau<sup>6</sup>, Adam Brazil<sup>7</sup>, Matthew A. Wood<sup>6</sup>, Stéphane Merlino<sup>8</sup>, Pierre-Jean Vazel<sup>9</sup>, and Ian N.  
8 Bezodis<sup>6</sup>  
9

10 **Affiliations:** <sup>1</sup>Carnegie School of Sport, Leeds Beckett University, Leeds, UK;  
11 <sup>2</sup>Athletics Biomechanics, Leeds, UK; <sup>3</sup>School of Sport and Exercise, University of  
12 Gloucestershire, Gloucester, UK; <sup>4</sup>Athletics Sector, School of Physical Education & Sport  
13 Science, National & Kapodistrian University of Athens, Athens, Greece; <sup>5</sup>European School of  
14 Physiotherapy, Amsterdam University of Applied Sciences, Amsterdam, The Netherlands;  
15 <sup>6</sup>Cardiff School of Sport and Health Sciences, Cardiff Metropolitan University, Cardiff, UK;  
16 <sup>7</sup>Department for Health, University of Bath, Bath, UK; <sup>8</sup>International Relations &  
17 Development Department, World Athletics, Monaco; <sup>9</sup>Athlétisme Metz Métropole, Metz,  
18 France.  
19

20 **Correspondence:** Athanassios Bissas, [a.bissas@athleticsbiomechanics.com](mailto:a.bissas@athleticsbiomechanics.com)  
21

22 **Text-only word count:** 3490  
23

24 **No. of figures & tables:** 4 figures, 3 tables  
25

26 **ABSTRACT: (243 words)**

27 The aim was to investigate the kinematic factors associated with successful performance in the  
28 initial acceleration phase of a sprint in the best male athletes in the World at the 2018 World  
29 Indoor Athletics Championships. High speed video (150 Hz) was captured for eight sprinters  
30 in the men's 60 m final. Spatio-temporal and joint kinematic variables were calculated from  
31 the set position to the end of the first ground contact post-block exit (GC1). Normalised average  
32 horizontal external power (NAHEP) defined performance and was the dependent variable for  
33 a series of regression analyses. Clear relationships were found between GC1 NAHEP and 10-  
34 m time, 60-m time, change in velocity, acceleration and contact time in the first ground contact  
35 ( $r = -0.74, -0.64, 0.96, 0.91$  and  $-0.56$ , respectively). Stepwise multiple linear regression of  
36 joint kinematic variables in the first ground contact revealed that trunk angle at take-off and  
37 thigh separation angle at take-off explained nearly 90% of variation in GC1 NAHEP ( $R^2 =$   
38  $0.89$ ). The athletes' projection at take-off with a forward leaning trunk and large thigh  
39 separation is characteristic therefore of excellent initial acceleration performance and this will  
40 be a good visual guide for technical coaching instruction. This was the first study of its kind to  
41 adopt such a research design in a World-class sample in a representative environment. Future  
42 studies that combine detailed kinematic and kinetic data capture and analysis in such a setting  
43 will add further insight to the findings of this investigation.

44

45 **Keywords:** acceleration, athletics, elite, power, running

46

47

48 **INTRODUCTION:**

49 The start and initial acceleration phase are of key importance to the short sprints ( $\leq 100$  m, Mero  
50 1988, Bezodis et al., 2015a), yet the biomechanical factors that distinguish performance in this  
51 phase at the very highest level of competition are not known. Given that the aim of the start  
52 and initial acceleration phase is to maximise horizontal velocity in the minimum possible time  
53 (Bezodis et al., 2019a), normalised average horizontal external power (NAHEP) has been  
54 proposed and justified as the criterion for successful performance early in the sprint (Bezodis  
55 et al., 2010; 2019a). NAHEP is therefore now widely used to define and distinguish effective  
56 acceleration performance in the sprint running biomechanics literature (e.g. Bezodis et al.,  
57 2015a; Otsuka et al., 2015; Willwacher et al., 2016; Brazil et al., 2018; Wild et al., 2018;  
58 Bezodis et al., 2020; Sado et al., 2020; Sandamas et al., 2020; von Lieres und Wilkau et al.,  
59 2020a).

60  
61 Perhaps because of the restrictions hindering researchers from investigating performance in  
62 elite competition, ecologically valid and detailed analyses of the biomechanics of the start and  
63 initial acceleration phase in World-class (sub-10 s personal best [PB]) male sprinters in  
64 competition are limited in the scientific literature (Bezodis et al., 2019a). Indeed, to the authors'  
65 knowledge only two such studies exist (Ciacci et al., 2017; Bezodis et al., 2019b). The first  
66 analysed spatio-temporal parameters post-block exit, finding that sprinters with faster PBs had  
67 longer contact times and shorter flight times than their slower counterparts (Ciacci et al., 2017).  
68 Secondly, Bezodis et al. (2019b) investigated differences in centre of mass (CM) translation  
69 between world-class sprinters and high hurdlers, yet did not consider factors that distinguished  
70 performance within either group.

71

72 On the other hand, studies of elite and sub-elite male athletes, but still below World-class  
73 standard (100 m PB approximately between 10 and 11 s), are more prevalent in the literature  
74 (for a comprehensive review see Bezodis et al., 2019a), and tend to be based on training or  
75 laboratory-based data. Within that broad performance classification, for the first step post block  
76 exit, better sprinters touch down and take-off with the CM further down the track, have a longer  
77 step length, and also a greater horizontal velocity at take-off (Slawinski et al., 2010a). A  
78 theoretical investigation showed that reducing the amount of ankle dorsiflexion early in the  
79 first stance phase can increase NAHEP in that ground contact (Bezodis et al., 2015b), yet  
80 despite three studies investigating the block phase and first flight (Bezodis et al., 2015a; Ciacci  
81 et al., 2017; Bezodis et al., 2019b), there is little other applied evidence in the literature that  
82 has shown which joint kinematic parameters play an important role in determining initial sprint  
83 acceleration performance post-block exit.

84

85 Therefore, there is a significant gap in the peer-reviewed sprinting literature preventing  
86 scientists and coaches from forming a complete understanding of the key mechanical factors  
87 governing the explosive movement of the body during the first step post-block exit. The most  
88 effective way to address this gap, so findings are ecologically valid, would be to derive data  
89 from a highly competitive environment including the very best sprinters in the world. Such  
90 data will provide an unprecedented insight into the mechanics of maximal human acceleration.  
91 Consequently, this study investigated the kinematic factors that were associated with successful  
92 performance in the initial acceleration phase of a sprint in a sample of the very best male  
93 athletes in the World at the highest possible competition level. Developing an understanding  
94 of those key factors will aid coaches and scientists in designing technical training programs to  
95 develop and facilitate optimal performance in elite athletes.

96

97 **METHODS:**

98 **Participants**

99 Data were collected as a part of the Birmingham 2018 IAAF World Indoor Championships  
100 Biomechanics Research Project (Walker et al., 2019). The use of the data for this study was  
101 approved by World Athletics (formerly known as IAAF), who own and control the data, and  
102 locally via institutional research ethics approval. The eight finalists of the men's 60 m race (25  
103  $\pm$  3 years, PB prior to the race:  $6.51 \pm 0.10$  s), who included the world record holder, were  
104 recorded on the evening of 3rd March 2018 at Arena Birmingham, UK. The race was the fastest  
105 of all men's 60 m races in the history of World Championships (World Athletics, 2020a) with  
106 three sprinters achieving sub-6.50 s times and the winner setting a new Championship Record  
107 (6.37 s).

108

109 **Data Collection and Processing**

110 All data collection and initial processing was carried out as previously described in Bezodis et  
111 al. (2019b, pp3-4 for more detail). Briefly, four Sony PXW-FS7 cameras operating at 150 Hz  
112 captured a three-dimensional volume covering the starting blocks to 5 m beyond the start line.  
113 Videos were processed in SIMI Motion (version 9.2.2, Simi Reality Motion Systems GmbH,  
114 Germany). To address the aim of this study, the analysis was focused on the following phases:  
115 a; block phase (from the onset of movement to the final frame of foot contact with the starting  
116 block), b; the subsequent flight phase (from the first frame after block exit to the final frame  
117 before ground contact), and c; the first ground contact post-block exit (GC1; from the first to  
118 the final visible frame of foot contact with the track). The onset of movement was defined via  
119 visual inspection of the first visible movement of the athlete in lane 8 using an additional Sony  
120 PXW-FS5 camera at close proximity, operating at 200 Hz. This camera was synchronised to

121 the other four cameras, and the official reaction times were used to calculate the onset of  
122 movement in the other athletes from the athlete in lane 8.

123

124 Shoulder, hip, knee, ankle and metatarsophalangeal joints were digitised continuously on the  
125 side of the rear leg in the blocks from the onset of movement in the block to the second  
126 touchdown. Additionally, a 17-point whole-body model was digitised at onset of movement,  
127 block clearance, and each subsequent take-off and touchdown event. Co-ordinates were  
128 reconstructed using the Direct Linear Transformation algorithm (Abdel-Aziz et al., 2015).  
129 Three dimensional co-ordinates were projected onto a two-dimensional sagittal plane for  
130 analysis. Segmental and whole body centres of mass were calculated according to de Leva  
131 (1996), and continuous joint centre coordinates were filtered with a recursive second-order,  
132 low-pass Butterworth filter (zero-phase lag), with cut-off frequencies calculated by residual  
133 analysis (Winter, 2009; mean value for all joint centres 13.4 Hz, range 10.0-15.5 Hz).

134

135 The dependent variable was GC1 NAHEP, calculated as described by Bezodis et al. (2010).  
136 Participants' body mass could not be directly measured because of the access granted for data  
137 collection. However, despite NAHEP normalising for body mass (based on the approach of  
138 Hof, 1996), mass itself is not required to perform the calculation (see appendix). For the block  
139 phase and GC1, the times between events (e.g. block time defined from first visible movement  
140 to block exit) were combined with CM horizontal displacements and used to calculate CM  
141 velocities, acceleration and NAHEP. Touchdown and take-off distances were calculated as the  
142 coordinate of the metatarsophalangeal joint of the contact foot minus the coordinate of the CM  
143 in the antero-posterior direction. Segment angles were defined with anticlockwise as positive  
144 relative to the global forward horizontal, and joint angles with extension as positive (see Figure  
145 1). Joint angular velocities were calculated as the differential of joint angle with respect to time.

146 Vertical and horizontal foot touchdown velocities were calculated as the differential of the  
147 respective segment CM displacement with respect to time. Thigh separation angle was defined  
148 as the difference between the segment angles of the thighs of the swing and ground contact  
149 legs.

150 \*\*\* Insert Figure 1 near here \*\*\*

151

## 152 **Statistical Analysis**

153 To assess the relationships between specific biomechanical data and first stance performance  
154 (GC1 NAHEP), Pearson correlation coefficients and 90% confidence intervals (using the  
155 Fisher  $z'$  method; Fisher, 1921) were calculated (Batterham & Hopkins, 2006). If the  
156 confidence intervals overlapped, i.e. completely crossed, the trivial threshold (−0.1 to 0.1)  
157 based on the smallest practically important correlation, the relationship was deemed unclear.  
158 For correlations deemed clear, the magnitude of the relationship was interpreted using the  
159 convention proposed by Hopkins (2016): moderate (0.30-0.49), large (0.50-0.69), very large  
160 (0.70-0.89) and practically perfect (0.90-1.00). To further investigate the segment and joint  
161 kinematic determinants of first stance performance, a stepwise multiple regression was  
162 performed (IBM SPSS Statistics, v. 22.0) using 0.1 as the criterion value of entry of a variable  
163 in the regression model, with the alpha level set at 0.05. Normality of the residuals was  
164 confirmed (Shapiro-Wilk = 0.93 for both standardised and unstandardised residuals), and there  
165 was minimal autocorrelation (Durbin-Watson = 2.103).

166

## 167 **RESULTS:**

168 Group mean  $\pm$  standard deviation (SD) block, 10-m and 60-m times were  $0.34 \pm 0.02$  s,  $1.91 \pm$   
169  $0.03$  s and  $6.51 \pm 0.10$  s, respectively (Table 1). Clear relationships were found between first  
170 stance performance and 10-m and 60-m times ( $r = -0.74$ , very large and  $-0.64$ , large,



171 respectively, Figure 2). After exiting the blocks with a horizontal velocity of  $4.28 \pm 0.35 \text{ m}\cdot\text{s}^{-1}$   
172 <sup>1</sup>, sprinters increased their running velocity on average by  $1.57 \pm 0.17 \text{ m}\cdot\text{s}^{-1}$  during first stance,  
173 in a ground contact time of  $0.175 \pm 0.014 \text{ s}$ . For data collected during GC1, change in CM  
174 velocity ( $r = 0.96$ , nearly perfect), CM acceleration ( $r = 0.91$ , nearly perfect) and contact time  
175 ( $r = -0.56$ , large) all possessed clear relationships with first stance performance. NAHEP  
176 during first stance ( $1.624 \pm 0.269$ ) was greater than that demonstrated in the block phase ( $0.953$   
177  $\pm 0.143$ ), with no clear relationship observed between the two ( $r = 0.12$ , Table 1, Figure 2).

178

179 \*\*\* Insert Table 1 near here \*\*\*

180 \*\*\* Insert Figure 2 near here \*\*\*

181

182 Of all kinematic variables quantified during first stance (Table 2), only thigh separation ( $r =$   
183  $0.62$ , large) and trunk ( $r = -0.59$ , large) angles at TO possessed a clear linear relationship with  
184 first stance performance (Figure 3). Individual scatter plots for all bivariate correlations deemed  
185 clear are presented in Figure 4. Following stepwise multiple regression analysis for kinematic  
186 data, two variables explained nearly 90% of the variance in first stance performance ( $R^2 =$   
187  $0.89$ ): thigh separation angle at take-off and trunk angle at take-off (Table 3).

188

189 \*\*\* Insert Table 2 near here \*\*\*

190 \*\*\* Insert Figure 3 near here \*\*\*

191 \*\*\* Insert Figure 4 near here \*\*\*

192 \*\*\* Insert Table 3 near here \*\*\*

193

194

195 **DISCUSSION:**

196 The aim of this study was to investigate the kinematic factors associated with successful  
197 performance in the initial acceleration phase of a sprint in the very best male athletes in the  
198 World. Based on the simple bivariate correlation analysis undertaken, the better performers in  
199 this study, defined by the power generated during the first ground contact post-block exit (GC1  
200 NAHEP), were quicker to both 10 and 60 m (Table 1, Figure 2). Additionally, those better  
201 performers increased their CM velocity more in a shorter contact time in GC1, thereby  
202 achieving a greater amount of CM acceleration during that ground contact (Table 1, Figure 2).  
203 This study then addressed the lack of previously published evidence regarding the influence of  
204 joint and segmental kinematics on elite initial acceleration sprint performance. Based on  
205 bivariate correlation analyses of the first stance (Table 2, Figure 3), trunk angle at take-off and  
206 thigh separation angle at take-off were found to be associated with GC1 NAHEP, and together  
207 they explained almost 90% of the variance in first stance performance (Table 3).

208

209 The scope for comparison with equivalent previous studies is limited because of the highly  
210 novel nature of this study. Ciacci et al. (2017) reported spatio-temporal variables for four  
211 World-class male sprinters with a mean 100 m PB of 10.03 s from a Diamond League event.  
212 Comparisons reveal shorter block times (0.342 vs. 0.356 s) and greater block clearance  
213 velocities (4.28 vs. 4.16 m·s<sup>-1</sup>) in the current study. Direct comparison between the two studies  
214 is difficult, since exact differences in athlete abilities and performance on the day relative to  
215 that are not possible to identify, and there could be further differences due to potential  
216 variations in data collection and processing. Other studies have reported values of block  
217 NAHEP of 0.53 ± 0.08 (Bezodis et al., 2015a), 0.539 ± 0.053 (Otsuka et al., 2015) and  
218 approximately 0.2-0.5 (Willwacher et al., 2016). These are clearly lower than the value of 0.953  
219 ± 0.143 reported here. There are two reasons for this. Firstly, the range of abilities of athletes

220 studied were much greater in the previous literature than here, despite the inclusion of some  
221 World-class athletes across the samples (100 m PB range; 9.98-11.6 s (Bezodis et al., 2015a),  
222 10.21-11.65 s (Otsuka et al., 2015), 9.58-14.00 s (Willwacher et al., 2016)). Secondly,  
223 Willwacher et al. (2016) normalised their data to height rather than leg length, due to the  
224 inclusion of a comparison with lower-limb amputee sprinters in their study. This has the effect  
225 of increasing the denominator in the NAHEP calculation, and therefore reducing the calculated  
226 value.

227

228 Bezodis et al. (2015a) reported a mean GC1 touchdown distance of  $-0.20 \pm 0.07$  m in 16 male  
229 sprinters with a range of 100 m PBs from 9.98 to 11.6 s. That investigation showed a mean foot  
230 position farther behind the CM than in the current study ( $-0.12 \pm 0.06$  m, Table 2), but in  
231 athletes of a much wider range of abilities than this study. Using a simulation modelling  
232 approach for an individual athlete with a 100 m PB of 10.28 s, Bezodis et al. (2015b) showed  
233 that the optimum touchdown distance in GC1 for the generation of NAHEP was approximately  
234  $-0.09$  m. That result is based on the specific individual characteristics of the athlete in question  
235 (such as leg length and stature) but suggests that there might be a similarly located optimum  
236 value for all sprinters. Bezodis et al. (2015b) used their simulation model to further show the  
237 importance of reducing ankle dorsiflexion angle in early GC1 stance to the generation of  
238 NAHEP, supporting the previous findings of Charalambous et al. (2012). The results of the  
239 current study showed a moderate but unclear contribution of dorsiflexion range of motion to  
240 GC1 NAHEP (Table 2). Further investigations in elite athletes that explore the role of the  
241 dorsiflexors in developing sprint acceleration in more detail are required.

242

243 Those athletes who were the most effective starters in this study adopted a body position at  
244 take-off from the first contact that was characterised by a large forward lean in the trunk and a

245 large amount of separation between the two thigh segments. It is highly likely that the body  
246 position at take-off of the most successful starters described here comes about as an effect of  
247 the successful ground contact that has preceded it, rather than being the cause of the high  
248 standard of performance in itself. Nevertheless, from a technical coaching perspective, a body  
249 position at GC1 take-off characterised by large forward trunk lean, and a large amount of thigh  
250 separation is likely to be a good visual marker of highly effective initial acceleration  
251 performance.

252

253 It is well established that effective maximal sprint acceleration is dependent upon the athlete  
254 adopting a primarily horizontal orientation of the resultant external force vector (Morin et al.,  
255 2011; Rabita et al., 2015). A study of 41 non-sprint trained physical education students (Kugler  
256 and Janshen, 2010) showed that the orientation of the external force vector at maximum force  
257 was highly correlated with body lean ( $r = 0.93$ ), and therefore that greater forward lean of the  
258 body resulted in greater propulsive forces. In the block start, Otsuka et al. (2014) showed that  
259 there was no difference in the magnitude of resultant force between well-trained (mean PB =  
260 10.87 s) and trained sprinters (mean PB = 11.31 s), but that the anteroposterior force component  
261 was greater and the angle of the resultant force more forward, in the well-trained sprinters.  
262 Further studies of the kinematics of the acceleration phase in well-trained sprinters have  
263 confirmed that the athletes' trunk angle raises throughout the sprint (Nagahara et al., 2014; von  
264 Lieres und Wilkau et al., 2020b) at the same time as the resultant force vector become more  
265 vertical (Morin et al., 2011). However, to the authors' knowledge there are currently no studies  
266 that comprehensively investigate the relationship between joint or segment kinematics and  
267 external kinetics throughout the initial acceleration phase in well-trained or elite sprinters. Such  
268 studies have the potential to be particularly revealing regarding the underlying mechanisms  
269 that dictate initial sprint acceleration performance in this population.

270 There is limited evidence available in the literature to support the finding here of the importance  
271 of thigh separation angle at take-off to sprint acceleration performance. However, there are two  
272 possible mechanisms that might be responsible. Firstly, the individual segments of the body  
273 each contribute to the overall kinetic energy of the athlete's body. Slawinski et al. (2010b)  
274 investigated segmental contributions during the block phase only. They showed that the thigh  
275 segments combined created more maximal kinetic energy than any other segments (thighs –  
276 156.1 J; thorax 142.5 J). In creating a large separation of the thighs at take-off in this study it  
277 is possible that the better starters are maximising the amount of kinetic energy created.  
278 Secondly, thigh angular velocity is thought to be an important component of sprint running.  
279 Clark et al. (2020) investigated maximum velocity trials and found strong positive relationships  
280 between thigh angular velocity and both lower limb velocity at touchdown and running speed.  
281 This suggests that the large thigh separation angle at take-off seen in this study might be putting  
282 the athletes in an effective position to create large thigh angular velocities in the swing phase  
283 immediately prior to the subsequent touchdown, to optimise the mechanics of the foot-ground  
284 interaction during that ground contact.

285

286 Overall, spatio-temporal data suggest that the change in CM velocity during GC1 was more  
287 important to the development of GC1 NAHEP than was the corresponding ground contact time  
288 ( $r = 0.96$ , nearly perfect, and  $-0.56$ , large, respectively, Table 1). This is supported by data  
289 from the block phase in 103 male and 51 female trained sprinters, presented by Willwacher et  
290 al. (2016), which showed  $r$  values across all 154 participants of 0.91 and 0.52 respectively for  
291 change in horizontal velocity and block time in relation to NAHEP. The importance of  
292 horizontal impulse to sprint acceleration performance is well established (Hunter et al., 2005;  
293 Morin et al., 2015). Impulse is the product of the force produced and the time taken to produce  
294 it and, when divided by body mass, equates to the change in velocity of the athlete. The spatio-

295 temporal results from this study and Willwacher et al. (2016) suggest that it could be the  
296 magnitude of the propulsive force rather than its duration that is the most important component  
297 in creating impulse, and therefore increasing velocity. This is supported by a recent study by  
298 von Lieres und Wilkau et al. (2020a), who used a commonality regression analysis to show  
299 that magnitude of the propulsive force was the largest contributor to NAHEP in the initial  
300 acceleration phase in 28 well-trained sprinters. Von Lieres und Wilkau et al. (2020a) did not  
301 include joint kinematics in their regression analysis, so further studies that combine detailed  
302 measures of kinematics and kinetics in the initial acceleration phase in well-trained and elite  
303 sprinters are necessary to investigate these relationships further.

304

305 The sample size here was limited by the nature of the data collection setting, but in keeping the  
306 participants to the very best male sprinters in the World, this study gives the first insight in the  
307 peer-reviewed literature into the factors that determine initial acceleration performance in elite  
308 sprinters in competition. Indeed, in the race studied here, the medallists ran three of the 20  
309 fastest times in the history of the event (World Athletics, 2020b). One possible outcome of that  
310 is that homogenous nature of the sample investigated here might have reduced the number of  
311 clear relationships found in the data. The benefit of focusing this novel analysis on the best  
312 sprinters in the World outweighs that risk, however. Further, the data collection environment  
313 precluded the capture of kinetic data, something that will remain unfeasible during official  
314 competitions due to the constraints imposed by the rules of the sport and technological  
315 complexities. However, this is the first study in the peer-reviewed literature to investigate the  
316 kinematic factors that determine performance in World-class male sprinters in the initial  
317 acceleration phase in elite competition. In doing so, it maintained a truly representative  
318 environment that ensured the integrity of the competitive task (i.e., the data collection took  
319 place during a World Indoor Championships final and did not interfere with the athletes'

320 performance in any way). As such, it provides an extremely useful insight into previously  
321 unreported aspects of performance in this otherwise widely studied skill (Bezodis et al., 2019a),  
322 which will provide a useful insight from an ecologically valid setting for coaches and technical  
323 analysts when looking to improve performance in other sprinters.

324

325 In conclusion, this study identified two key joint kinematic variables that were associated with  
326 initial acceleration performance in World-class male sprinters in the World Indoor  
327 Championships final of 2018. Those two variables were trunk angle and thigh separation angle  
328 at take-off, and they are likely to provide a good visual guide to coaches and scientists when  
329 attempting to identify the technical characteristics of successful initial acceleration technique.

330

#### 331 **ACKNOWLEDGEMENTS:**

332 The authors would like to thank SEIKO Timing Services for accommodating our data  
333 collection requests.

334

#### 335 **CONFLICT OF INTEREST STATEMENT:**

336 The authors have no conflicts of interest that are relevant to the findings of this manuscript.

337

#### 338 **SOURCES OF FUNDING:**

339 The data collection and initial data analysis were supported by funding provided by the IAAF  
340 / World Athletics as part of a wider development / education project; however, the nature of  
341 the data is purely descriptive and not associated with any governing body, commercial sector  
342 or product. No funding was provided for the writing of this manuscript. The results of the  
343 present study do not constitute endorsement by World Athletics.

344

345 **REFERENCES:**

- 346 Abdel-Aziz, Y. I., Karara, H. M., Hauck, M., 2015. Direct linear transformation from  
347 comparator coordinates into space coordinates in close-range photogrammetry.  
348 Photogrammetric Engineering & Remote Sensing 81, 103-107.
- 349 Batterham, A. M., Hopkins, W.G., 2006. Making meaningful inferences about magnitudes.  
350 International Journal of Sports Physiology and Performance 1, 50-57.
- 351 Bezodis, I. N., Brazil, A., von Lieres und Wilkau, H. C., Wood, M. A., Paradisis, G. P., Hanley,  
352 B., Tucker, C. B., Pollitt, L., Merlino, S., Vazel, P.-J., Walker, J., Bissas, A., 2019b. World-  
353 Class Male Sprinters and High Hurdlers Have Similar Start and Initial Acceleration  
354 Techniques. Frontiers In Sports and Active Living 1(23), doi: 10.3389/fspor.2019.00023.
- 355 Bezodis, I. N., Cowburn, J., Brazil, A., Richardson, R., Wilson, C., Exell, T. A., Irwin, G.,  
356 2020. A biomechanical comparison of initial sprint acceleration performance and technique in  
357 an elite athlete with cerebral palsy and able-bodied sprinters. Sports Biomechanics 19, 189-  
358 200.
- 359 Bezodis, N. E., Salo, A. I. T., Trewartha, G., 2010. Choice of sprint start performance measure  
360 affects the performance-based ranking within a group of sprinters: which is the most  
361 appropriate measure? Sports Biomechanics 9, 258-269.
- 362 Bezodis, N. E., Salo, A. I. T., Trewartha, G., 2015a. Relationships between lower-limb  
363 kinematics and block phase performance in a cross section of sprinters. European Journal of  
364 Sport Science 15, 118-124.
- 365 Bezodis, N. E., Trewartha, G., Salo, A. I. T., 2015b. Understanding the effect of touchdown  
366 distance and ankle joint kinematics on sprint acceleration performance through computer  
367 simulation. Sports Biomechanics 14, 232-245.
- 368 Bezodis, N. E., Willwacher, S., Salo, A. I. T., 2019a. The Biomechanics of the Track and Field  
369 Sprint Start: A Narrative Review. Sports Medicine 49, 1345-1364.



370 Brazil, A., Exell, T., Wilson, C., Willwacher, S., Bezodis, I. N., Irwin, G., 2018. Joint kinetic  
371 determinants of starting block performance in athletic sprinting. *Journal of Sports Sciences* 36,  
372 1656-1662.

373 Charalambous, L., Irwin, G., Bezodis, I. N., Kerwin, D., 2012. Lower limb joint kinetics and  
374 ankle joint stiffness in the sprint start push-off. *Journal of Sports Sciences* 30, 1-9.

375 Ciacci, S., Merni, F., Bartolomei, S., Di Michele, R., 2017. Sprint start kinematics during  
376 competition in elite and world-class male and female sprinters. *Journal of Sports Sciences* 35,  
377 1270-1278.

378 Clark, K. P., Meng, C. R., Stearne, D. J., 2020. ‘Whip from the hip’: thigh angular motion,  
379 ground contact mechanics and running speed. *Biology Open* 9, bio053546.

380 de Leva, P., 1996. Adjustments to Zatsiorsky-Seluyanov's segment inertia parameters. *Journal*  
381 *of Biomechanics* 29, 1223-1230.

382 Fisher, R. A. (1921). On the probable error of a coefficient of correlation deduced from a small  
383 sample. *Metron*, 1, 3–32.

384 Hof, A. L., 1996. Scaling gait data to body size. *Gait & Posture* 4, 222-223.

385 Hopkins, W.G., 2016. A scale of magnitudes for effect statistics. Retrieved from  
386 <http://www.sportsci.org/resource/stats/>

387 Hunter, J. P., Marshall, R. N., McNair, P. J., 2005. Relationships between ground reaction force  
388 impulse and kinematics of sprint-running acceleration. *Journal of Applied Biomechanics* 21,  
389 31-43.

390 Kugler, F., Janshen, L., 2010. Body position determines propulsive forces in accelerated  
391 running. *Journal of Biomechanics* 43, 343-348.

392 Mero, A., 1988. Force-Time Characteristics and Running Velocity of Male Sprinters During  
393 the Acceleration Phase of Sprinting. *Research Quarterly for Exercise and Sport* 59(2), 94-98.

394 Morin, J.-B., Edouard, P., Samozino, P., 2011. Technical Ability of Force Application as a  
395 Determinant Factor of Sprint Performance. *Medicine & Science in Sports & Exercise* 43, 1680-  
396 1688.

397 Morin, J.-B., Slawinski, J., Dorel, S., Saez de Villareal, E., Couturier, A., Samozino, P.,  
398 Brughelli, M., Rabita, G., 2015. Acceleration capability in elite sprinters and ground impulse:  
399 Push more, brake less? *Journal of Biomechanics* 48, 3149-3154.

400 Nagahara, R., Matsubayashi, T., Matsuo, A., Zushi, K., 2014. Kinematics of transition during  
401 human accelerated sprinting. *Biology Open* 3, 689-699.

402 Otsuka, M., Shim, J. K., Kurihara, T., Yoshioka, S., Nokata, M., Isaka, T., 2014. Effect of  
403 Expertise on 3D Force Application During the Starting Block Phase and Subsequent Steps in  
404 Sprint Running. *Journal of Applied Biomechanics* 30, 390-400.

405 Otsuka, M., Kurihara, T., Isaka, T., 2015. Effect of a Wide Stance on Block Start Performance  
406 in Sprint Running. *PLOS ONE* 10(11), e0142230.

407 Rabita, G., Dorel, S., Slawinski, J., Sàez-de-Villarreal, E., Couturier, A., Samozino, P., Morin,  
408 J. B. 2015. Sprint mechanics in world-class athletes: a new insight into the limits of human  
409 locomotion. *Scandinavian Journal of Medicine & Science in Sports* 25, 583-594.

410 Sado, N., Yoshioka, S., Fukashiro, S., 2020. Three-dimensional kinetic function of the lumbo-  
411 pelvic-hip complex during block start. *PLOS ONE* 15(3), e0230145.

412 Sandamas, P., Gutierrez-Farewik, E. M., Arndt, A., 2020. The relationships between pelvic  
413 range of motion, step width and performance during an athletic sprint start. *Journal of Sports*  
414 *Sciences* 38, 2200-2207.

415 Slawinski, J., Bonnefoy, A., Leveque, J. M., Ontanon, G., Riquet, A., Dumas, R., Cheze, L.,  
416 2010a. Kinematic and kinetic comparisons of elite and well-trained sprinters during sprint start.  
417 *Journal of Strength and Conditioning Research* 24, 896-905.

418 Slawinski, J., Bonnefoy, A., Ontanon, G., Leveque, J. M., Miller, C., Riquet, A., Cheze, L.,  
419 Dumas, R., 2010b. Segment-interaction in sprint start: Analysis of 3D angular velocity and  
420 kinetic energy in elite sprinters. *Journal of Biomechanics* 43, 1494-1502.

421 von Lieres und Wilkau, H. C., Bezodis, N. E., Morin, J.-B., Irwin, G., Simpson, S., Bezodis, I.  
422 N., 2020a. The importance of duration and magnitude of force application to sprint  
423 performance during the initial acceleration, transition and maximal velocity phases. *Journal of*  
424 *Sports Sciences* 38, 2359-2366.

425 von Lieres und Wilkau, H. C., Irwin, G., Bezodis, N. E., Simpson, S., Bezodis, I. N., 2020b.  
426 Phase analysis in maximal sprinting: an investigation of step-to-step technical changes between  
427 the initial acceleration, transition and maximal velocity phases. *Sports Biomechanics* 19, 141-  
428 156.

429 Walker, J., Tucker, C.B., Paradisis, G.P., Bezodis, I., Bissas, A., and Merlino, S., 2019.  
430 Biomechanical Report for the IAAF World Indoor Championships 2018: 60 Metres Men.  
431 Birmingham, UK: International Association of Athletics Federations.

432 Wild, J. J., Bezodis, I. N., North, J. S., Bezodis, N. E., 2018. Differences in step characteristics  
433 and linear kinematics between rugby players and sprinters during initial sprint acceleration.  
434 *European Journal of Sport Science* 18, 1327-1337.

435 Willwacher, S., Herrmann, V., Heinrich, K., Funken, J., Strutzenberger, G., Goldmann, J.-P.,  
436 Braunstein, B., Brazil, A., Irwin, G., Potthast, W., Brüggemann, G.-P., 2016. Sprint Start  
437 Kinetics of Amputee and Non-Amputee Sprinters. *PLoS ONE* 11(11), e0166219.

438 Winter, D. A., 2009. *Biomechanics and Motor Control of Human Movement*. John Wiley and  
439 Sons, Inc, Hoboken, NJ.

440 World Athletics, 2020a. Events Calendar: World Athletics Indoor Championships All Time.  
441 Retrieved from <https://www.worldathletics.org/competition/calendar->

442 results?disciplineId=4&permitLevelId=2&hideCompetitionsWithNoResults=true&competiti  
443 onGroupId=12  
444 World Athletics, 2020b. Senior Indoor 60 Metres Men: All Time Top List. Retrieved from  
445 [https://www.worldathletics.org/records/all-time-toplists/sprints/60-](https://www.worldathletics.org/records/all-time-toplists/sprints/60-metres/indoor/men/senior?regionType=world&timing=electronic&page=1&bestResultsOnly=false&firstDay=1900-01-01&lastDay=2020-09-15)  
446 [metres/indoor/men/senior?regionType=world&timing=electronic&page=1&bestResultsOnly](https://www.worldathletics.org/records/all-time-toplists/sprints/60-metres/indoor/men/senior?regionType=world&timing=electronic&page=1&bestResultsOnly=false&firstDay=1900-01-01&lastDay=2020-09-15)  
447 [=false&firstDay=1900-01-01&lastDay=2020-09-15](https://www.worldathletics.org/records/all-time-toplists/sprints/60-metres/indoor/men/senior?regionType=world&timing=electronic&page=1&bestResultsOnly=false&firstDay=1900-01-01&lastDay=2020-09-15)  
448

449 **APPENDIX:**

450 Average horizontal external power ( $\bar{P}$ ) is calculated based on the rate of change of kinetic  
451 energy with respect to time in the horizontal (antero-posterior) direction (Bezodis et al., 2010);

452 
$$\bar{P} = \frac{m(v_f^2 - v_i^2)}{2 \cdot \Delta t}$$

453 Where  $v_i$  and  $v_f$  are the horizontal velocities at the start and end of the push phase, respectively,  
454  $m$  is the mass of the sprinter and  $\delta t$  is the duration of the push phase.

455

456 Normalised average horizontal external power (NAHEP) is then calculated based on a  
457 modification of the function presented by Hof (1996), to obtain a dimensionless normalised  
458 power value (Bezodis et al., 2010);

459 
$$NAHEP = \frac{\bar{P}}{m \cdot g^{3/2} \cdot l^{1/2}}$$

460 Where  $g$  is acceleration due to gravity, and  $l$  is some measure of length or height, in the case  
461 of this study, the sum of the length of shank and thigh segments of each athlete taken from the  
462 reconstructed data (mean value = 0.843 m).

463

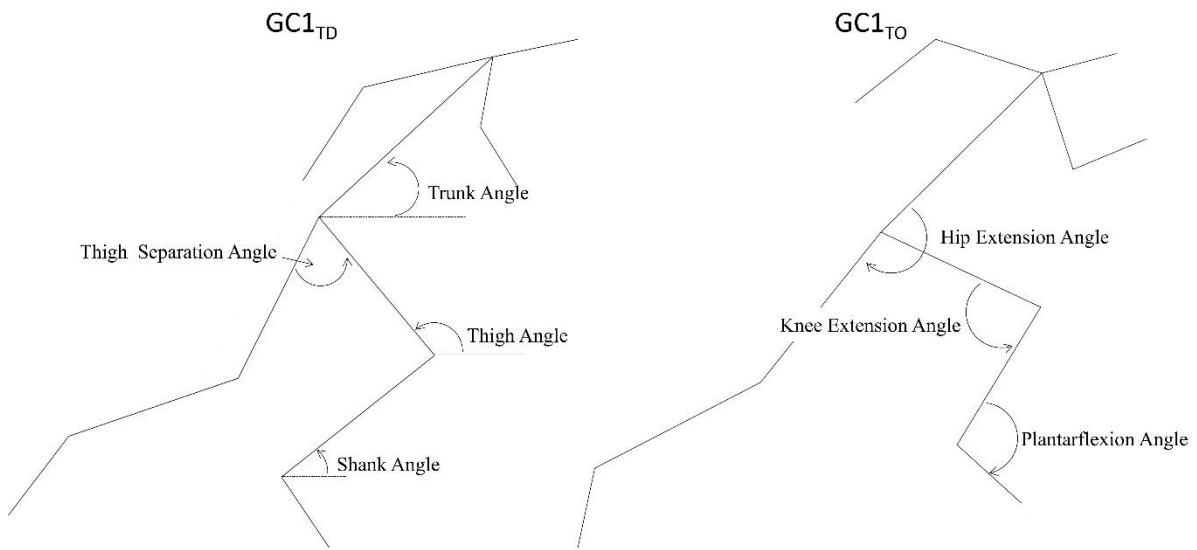
464 Therefore,  $NAHEP$  can be calculated when body mass is not known, thus;

465 
$$NAHEP = \frac{(v_f^2 - v_i^2)}{2\Delta t \cdot g^{3/2} \cdot l^{1/2}}$$

466

467

468 **FIGURES:**

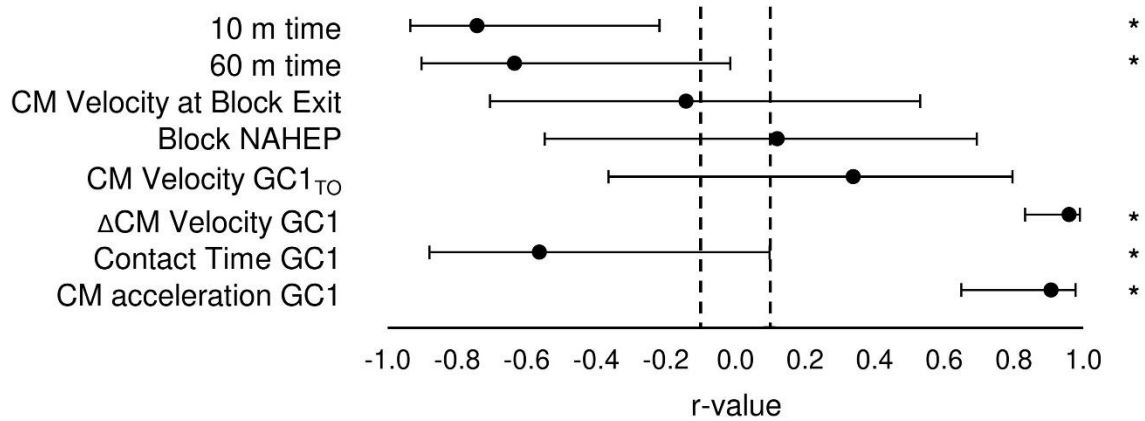


469

470 Figure 1. Spatial model showing mean scaled body positions across all athletes at the key events

471 GC1<sub>TD</sub> and GC1<sub>TO</sub>, and joint and segmental angular kinematic definitions.

472



473

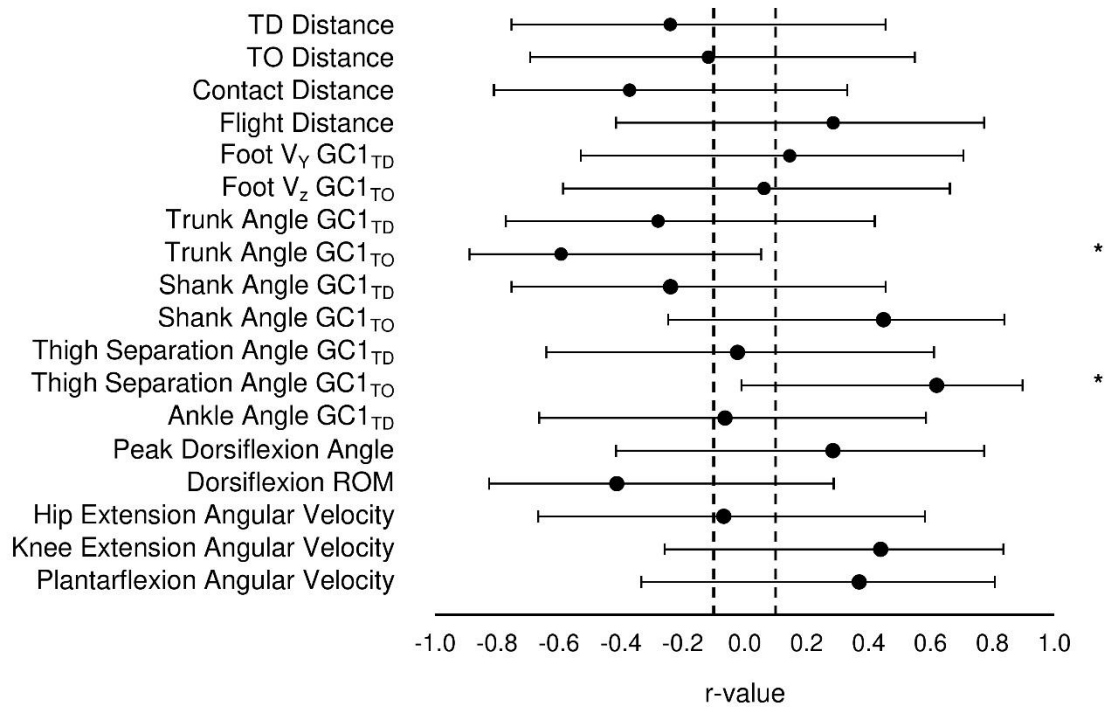
474 Figure 2. Correlation coefficients ( $\pm$  90% CI) between first stance performance (GC1 NAHEP)

475 and global biomechanical parameters. \* denotes CI does not cross the trivial zone ( $r = -0.1$  to

476 0.1).

477

478



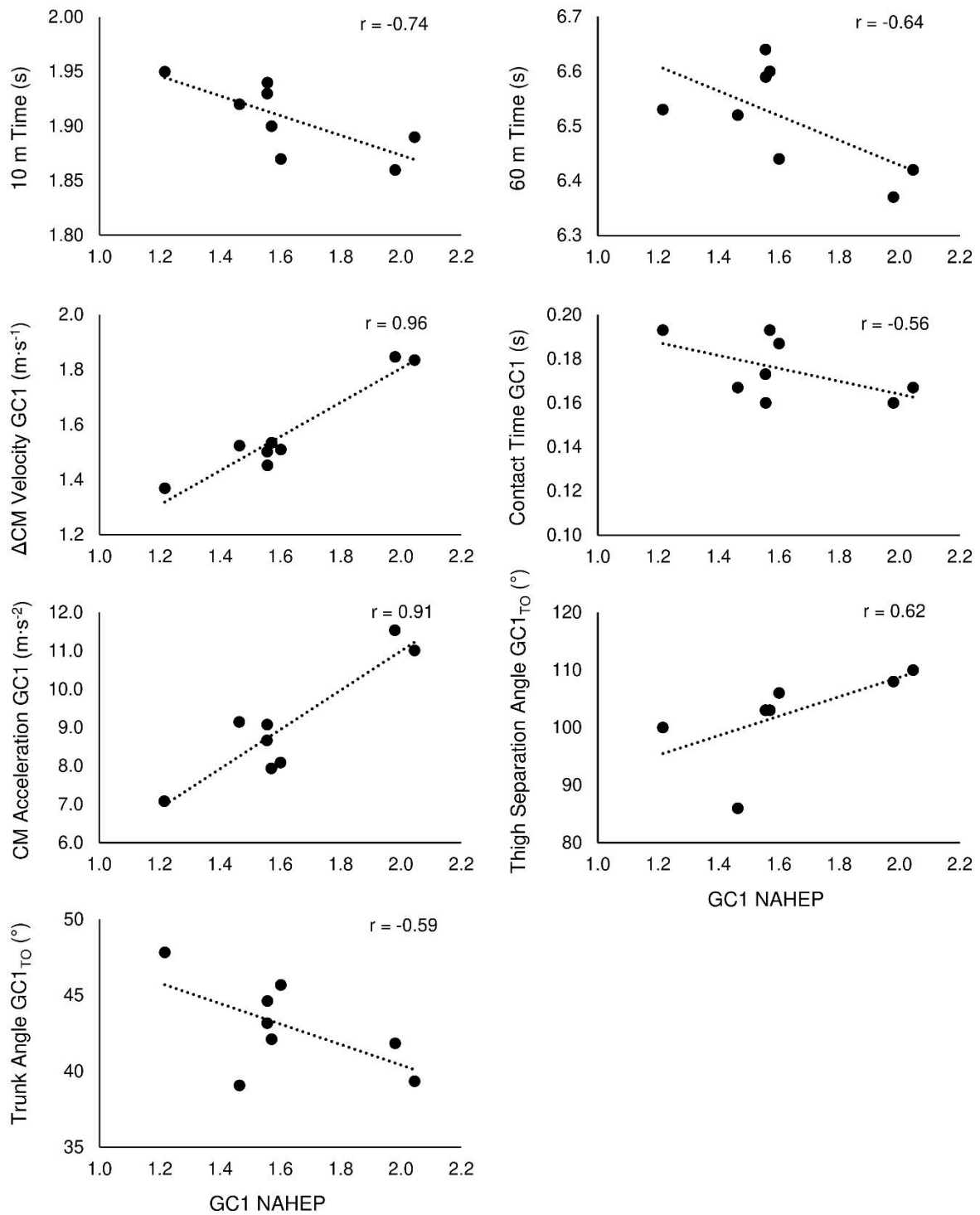
479

480 Figure 3. Correlation coefficients ( $\pm$  90% CI) between first stance performance (GC1 NAHEP)

481 and linear and angular kinematic variables. \* denotes CI does not cross the trivial zone ( $r = -$

482 0.1 to 0.1).

483



484

485 Figure 4. Individual correlation scatter plots for those variables with a clear correlation with

486 GC1 NAHEP.

487



488 **TABLES:**

489 Table 1. Global biomechanical parameters.

| Variable                                           | Mean    | SD    | r-value |
|----------------------------------------------------|---------|-------|---------|
| 10-m time (s)                                      | 1.91 ±  | 0.03  | -0.74 * |
| 60-m time (s)                                      | 6.51 ±  | 0.10  | -0.64 * |
| Block Time (s)                                     | 0.34 ±  | 0.02  | N/A     |
| CM Velocity at Block Exit (m·s <sup>-1</sup> )     | 4.28 ±  | 0.35  | -0.14   |
| Block NAHEP                                        | 0.953 ± | 0.143 | 0.12    |
| CM Velocity GC1 <sub>TO</sub> (m·s <sup>-1</sup> ) | 5.85 ±  | 0.35  | 0.34    |
| ΔCM Velocity GC1 (m·s <sup>-1</sup> )              | 1.57 ±  | 0.17  | 0.96 *  |
| Contact Time GC1 (s)                               | 0.175 ± | 0.014 | -0.56 * |
| CM acceleration GC1 (m·s <sup>-2</sup> )           | 9.07 ±  | 1.52  | 0.91 *  |
| GC1 NAHEP                                          | 1.624 ± | 0.269 |         |

490 *Note: r-value is the Pearson correlation coefficient with GC1 NAHEP. \* denotes a clear*  
 491 *correlation.*

492

493

494 Table 2. Kinematic data relating to first stance (GC1)

| Variable                                                  | Mean         | SD | r-value |
|-----------------------------------------------------------|--------------|----|---------|
| TD Distance (m)                                           | -0.12 ± 0.06 |    | -0.24   |
| TO Distance (m)                                           | -0.87 ± 0.03 |    | 0.12    |
| Contact Distance (m)                                      | 0.74 ± 0.07  |    | -0.37   |
| Flight Distance (m)                                       | 0.43 ± 0.06  |    | 0.29    |
| Foot $V_y$ GC1 <sub>TD</sub> (m·s <sup>-1</sup> )         | 0.24 ± 0.86  |    | 0.15    |
| Foot $V_z$ GC1 <sub>TD</sub> (m·s <sup>-1</sup> )         | -1.64 ± 0.41 |    | 0.06    |
| Trunk Angle GC1 <sub>TD</sub> (°)                         | 39 ± 3       |    | -0.28   |
| Trunk Angle GC1 <sub>TO</sub> (°)                         | 43 ± 3       |    | -0.59 * |
| Shank Angle GC1 <sub>TD</sub> (°)                         | 35 ± 3       |    | -0.24   |
| Shank Angle GC1 <sub>TO</sub> (°)                         | 26 ± 3       |    | 0.45    |
| Thigh Separation Angle GC1 <sub>TD</sub> (°)              | -70 ± 15     |    | -0.02   |
| Thigh Separation Angle GC1 <sub>TO</sub> (°)              | 102 ± 7      |    | 0.62 *  |
| Ankle Angle GC1 <sub>TD</sub> (°)                         | 87 ± 8       |    | -0.06   |
| Peak Dorsiflexion Angle (°)                               | 74 ± 5       |    | 0.29    |
| Dorsiflexion ROM (°)                                      | 14 ± 7       |    | -0.41   |
| Peak Hip Extension Angular Velocity (°·s <sup>-1</sup> )  | 202 ± 41     |    | -0.07   |
| Peak Knee Extension Angular Velocity (°·s <sup>-1</sup> ) | 169 ± 20     |    | 0.44    |
| Peak Plantarflexion Angular Velocity (°·s <sup>-1</sup> ) | 395 ± 95     |    | 0.37    |

495 *Note: r-value is the Pearson correlation coefficient with GC1 NAHEP. \* denotes a clear*  
 496 *correlation.*

497

498 Table 3. Angular kinematic regression model for first stance performance (GC1 NAHEP)

| Model                     |                                            | Unstandardised Coefficients | 95% CI           | Standardised Beta Coefficients |
|---------------------------|--------------------------------------------|-----------------------------|------------------|--------------------------------|
| Dependent:                | GC1 NAHEP                                  | Con. 1.434                  | 0.495 to 4.406   |                                |
| Independent(s)            |                                            | 0.027                       | 0.013 to 0.041   | 0.748                          |
| :                         | Thigh Separation Angle GC1 <sub>TO</sub> * |                             |                  |                                |
| R <sup>2</sup> = 0.89     | Trunk Angle GC1 <sub>TO</sub> *            | -0.061                      | -0.093 to -0.029 | -0.725                         |
| R <sup>2</sup> Adj = 0.85 |                                            |                             |                  |                                |

499 \* denotes significant ( $p < 0.05$ ) contribution to the regression model.

500